Chapter 4

D-shaped AZO coated low RI detection optical fiber SPR sensor

In this chapter, simulation of surface plasmon resonance (SPR) based Al-doped ZnO (AZO) coated long-range low refractive index detections in infrared range sensor by the finite element method (FEM) is presented. Plasmonic material Al-doped ZnO used for SPR condition in the desired range. The effect of thickness of the AZO layers on resonance wavelength, confinement loss, and sensitivity of the proposed sensor has been examined for different analyte refractive index (RI). These parameters do not change with AZO layers width variation. I have optimized coated AZO layer thickness 90 nm and width 124.70 μm in my work. The proposed infrared sensor has achieved RI sensitivity 2000-16000 nm/RIU and resolution $5.00 \times 10^{-5} - 6.25 \times 10^{-6}$ *RIU for refractive index of analyte range from 1.23 to 1.37. The proposed sensor is useful for detection of low RI organic chemical, biomedical, liquid foods and may be used other analyte sensing applications.*

4.1 Introduction

From the last three decades, the surface plasmon resonance (SPR) principle is more prevalent in detection of organic chemicals, bio-chemical, gases and other analyte. SPR based optical fiber devices have simple structure, small size, fast response, very sensitive, free-labelling, long-distance transmission and other unique properties[142]. A surface plasmon is a collective oscillation of free electrons charge density which is excited by the incident photons and propagates along the interface between metal and dielectric[143]. The SPR condition occurs, when propagation wave vector of incident photons and free electrons on the metal layer are matched together. In this condition a sharp resonance peak appears at a particular wavelength that wavelength is called resonance wavelength. The surface plasmon wave (SPW) is highly sensitive because that changes with the small change of refractive index of the analyte[144 145]. The SPR phenomena is very attractive for sensing application because of the extremely sensitive to change in refractive indices of the external medium. This aspect to useful in a different field such as medical diagnostics, biochemistry, biological substance, solution concentration measurement, food safety and environment monitoring[146 147 148 149 150]. The SPR technique based sensor also sensitive in diseases detection devices fields like as glucose detection in the urine, formalin detection in the food items, cancer cell and other viruses detection[151 152 153].

Conventional photonic crystal fiber[154] optical waveguide[155] and prism-metal coated[47 156 157] SPR based sensors are either too heavy or too complicated to operate in the actual condition. Optical fiber offers sensing devices which show more advantages i.e. simple and flexible design, small size, proper mode guide mechanism and extreme sensitivity. Sarika Shukla et al.[77] proposed a metal-ZnO bi layer SPR based fibre optic sensor which detects the analyte RIs range from 1.30 to 1.37. The maximum sensitivity was obtained 3161 nm/RIU in wavelengths range between 400 nm and 800 nm. R. Kanmani et al.[158]

had designed bi-layer silver (Ag) and titanium oxide (TiO_2) coated optical fiber sensor for isopropyl alcohol detection that work within wavelength range 900-1500 nm. The RIs of solution varies from 1.33 to 1.3597 with different concentration (0-60%) of isopropyl alcohol in distilled water. Bing-Hong Liu et al.[122] had proposed the experimental SPR based silver deposited hollow fibre (HF) sensor for detection of different volume ratios mixed solutions of kerosene and phonymethylphenyl siloxane liquid. Its liquid mixture solutions RI have range 1.51 - 1.58. This HF sensor achieved the highest sensitivity 6607 nm/RIU and resolution 0.8×10^{-4}- 2.5×10^{-4} RIU in wavelengths range 400-800 nm. B. Karki et al.[159] had proposed the multi layers metal and oxides coated surface plasmon biosensor. This biosensor is achieved the maximum sensitivity 664.6 °/ RIU at RI 1.37. J. K. Nayak et al.[78] had reported a D-shape SPR based silver-graphene coated fibre sensor for analyte RIs from 1.33 to 1.37 within wavelengths range from 600 nm to 900 nm. The maximum sensitivity and resolution of the sensor are 6800 nm/RIU and 8.0×10^{-5} RIU, respectively. Thus, most of the fibre sensors are detect the only high RI analyte within visible-infrared regions. Some substances have low RI such as fluorine-containing organics, liquid CO_2, medical oxygen[76] sevoflurane serving as anaesthetics in the medical field[160] [161] and other analytes. Therefore, to detect low RI analyte by the optical fiber sensor in the infrared region is the need of the day.

I have seen that zinc oxide (ZnO) is doped with aluminum (Al) for the enhancement of magnetic, electric and optical properties. Other group III metals like Boron (B), Gallium (Ga) and Indium (In) increase the properties of ZnO. The Al-O (0.192 nm) covalent bonding length is more close to that of Zn-O (0.197 nm) so Al-doped ZnO (AZO) is high conductive all of them[162]. Sensing devices are mainly depends on the plasmonic metals and their layers thickness. Plasmonic metals Copper (Cu), Silver (Ag) and Gold (Au) are the most commonly used to initiate SPPs for SPR condition[163]. Compared to these metals,

AZO is more available at a lower cost and has controllable conductive and optoelectric properties. Plasma frequency of AZO is lies in the near-infrared wavelength range[164]. Some authors proposed the experimentally and theoretically AZO coated optical fibre based sensors for different applications i.e. CO gas sensor[160], sodium acetate detection sensor, formaldehyde detection sensor, isopropyl alcohol with glycerin detection sensor[165] and relative humidity detection sensors[166 167].

In this work, I have proposed AZO coated D-shape single-mode optical fibre sensor based on SPR condition in IR region. The analysis has done by the finite element method (FEM) using the COMSOL Multiphysics software. By tuning the thickness and width of the AZO layers, the wavelength sensitivity of the sensor is obtained 2000-16000 nm/RIU for analyte RIs ranges 1.23-1.37, corresponding maximum resolution of 6.25×10^{-6} RIU within IR wavelength region.

4.2 Methodology

Fig.4.1 (a), (b) and (c) show the cross-section view, side view and set-up diagram of D-shaped AZO coated infrared sensor, respectively. In Fig. 4.1(a), grey, blue, red and green color shapes represent the fiber core, fiber cladding, Al-doped ZnO layer and analyte layer, respectively. Core with 8.2 μm diameter and 125 μm cladding diameter step-index single-mode optical fibre has been used for my simulation work. Germanium (Ge) doped silica and fluorine (F) doped silica have been used in fibre core and cladding respectively. The wavelength dependent RI of the core and cladding have measured by sellmeier's formula[102]

$$n^2(\lambda) = 1 + \frac{p_1\lambda^2}{\lambda^2 - q_1^2} + \frac{p_2\lambda^2}{\lambda^2 - q_2^2} + \frac{p_3\lambda^2}{\lambda^2 - q_3^2} \tag{4.1}$$

Where p_1, p_2, p_3, q_1, q_2, q_3 are sellmeier's coefficients and λ (in μm) is light source wavelength. Coefficients values of 4% Ge doped silica are $p_1 = 0.6867$, $p_2 = 0.4348$, $p_3 = 0.8966$, $q_1 = 0.07268$ μm, $q_2 = 0.1151$ μm, and $q_3 = 10.00$ μm and 1% F doped silica coefficients are p_1=0.696166, $p_2 = 0.407942$, $p_3 = 0.897479$, $q_1 = 0.068404$ μm, $q_2 = 0.116241$ μm, and $q_3 = 9.89616$ μm[75]. Using the Eq. (4.1), I plotted the dispersion spectra of fibre core and cladding which is shown in Fig. 4.2(a).

I have deposited AZO layer on the etched flat D-shaped optical fibre surface. The AZO layer is used as a plasmonic material for SPR condition. I have analyzed the sensor results for 30 to 90 nm thick AZO layers with 20 nm step increment. For AZO, dispersion spectra is defined by the following Drude model[168]

$$\epsilon = \epsilon_\infty - \frac{\omega_p^2}{(\omega^2+\gamma^2)} + \frac{i\gamma\omega_p^2}{\omega(\omega^2+\gamma^2)} \tag{4.2}$$

Where ϵ_∞(= 3.5) is represent the background permittivity, γ (= 4.86 × 10^{13} Hz) is the damping frequency and ω_p (= 5.22 × 10^{14} Hz) is the plasma frequency. Here $\omega = \frac{c}{\lambda}$, where c and λ are the speed of light and wavelength, respectively. Fig.2 (b) indicates the dispersion curve of AZO metal oxide that has obtained using the Drude model Eq. (4.2).

For analyzing the performance of the sensor, I have required the analytes in the external medium which are contact to the AZO layer. I have taken 20 μm thick analyte medium layer on the AZO layer in my model. In this work, I have analyzed the all modes for analytes RIs range from 1.23 to 1.37. The dielectric constant (ε_{am}) and refractive index (n_{am}) of the analyte have the relation $\varepsilon_{am} = n_{am}^2$. The excited surface plasmon wave (SPW) resonance condition is explained by the Eq. (4.3)[77].

$$\frac{2\pi}{\lambda} n_0 \, sin\alpha = Re(K_{spw}) \tag{4.3}$$

Where $K_{spw} = \frac{\omega}{c}\sqrt{\frac{\varepsilon_{AZO}\,\varepsilon_{am}}{\varepsilon_{AZO}+\varepsilon_{am}}} = \frac{2\pi}{\lambda}\sqrt{\frac{\varepsilon_{AZO}n_{am}^2}{\varepsilon_{AZO}+n_{am}^2}}$ is represents the propagation constant of the SPW and n_0 and c denote the fibre core RI and light velocity, respectively. Eq.(4.3) left side represents the propagation constant of the incident light source at wavelength λ at an angle α and right hand side Eq.(4.3) describes the propagation constant real value of the SPW. In right side Eq.(4.3), propagation constant is changed due to changing the analyte refractive index and therefore every RIs satisfied resonance condition at particular wavelength. The changed in analyte RI can be obtained by the resonance wavelength shifting. All used parameters in my designed structure are shown in the table (4.1).

Table 4.1 Used parameters values in the fibre sensor model.

Parameter	SI unit
fiber core diameter	8.2 μm
Fibre cladding diameter	125 μm
Optimized AZO layer thickness (t)	90 nm
Optimized AZO layer width (w)	124.57 μm
Taking analyte thickness	20 μm

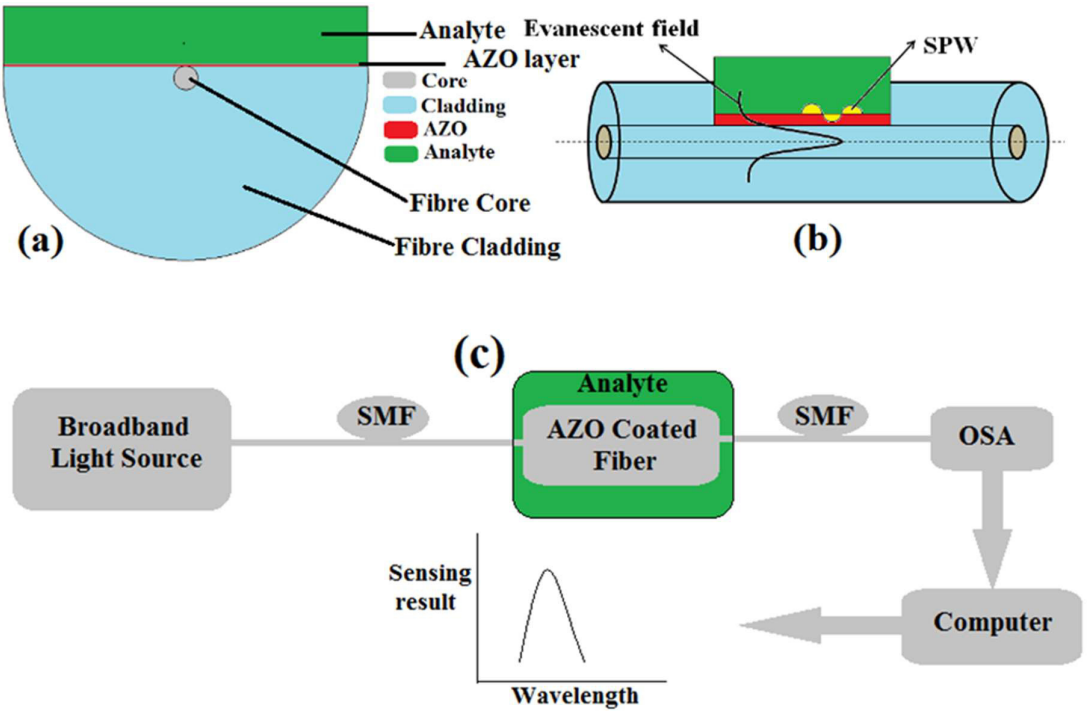

Fig. 4.1 Schematic diagram of D-shape AZO coated SPR based optical fiber sensor **(a)** Cross-section view **(b)** Side view **(c)** set-up diagram.

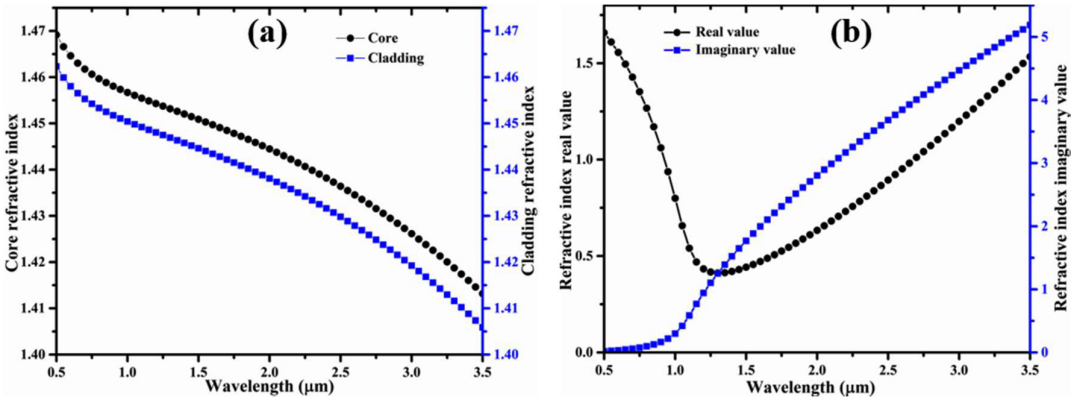

Fig. 4.2 Dispersion curves for **(a)** fiber core and cladding, and **(b)** Al-doped ZnO.

4.3 Result and Discussion

The fibre sensor modes characteristics have analyzed by the finite element method (FEM) using COMSOL multiphysics software. Figs. 4.3(a) and 4.3(b) illustrate the energy distribution of the core guided mode and SPP mode, respectively for analyte RI 1.23. Overall optical energy encloses in the core of fibre for core mode condition and in case of

SPP mode, energy presents on the AZO layer and in analyte medium. The Coupled mode phase-matching condition is satisfy, when the core mode and the SPP mode are drastically coupled and more energy transfer from core mode to the analyte medium. This SPR condition field energy distribution is shown in the Fig. 4.3(c).

The confinement loss or propagation loss is obtained by the following Eq. (4.4)[169]

$$Loss = \frac{54.5757 \times Im(n_{eff}) \times 10^4}{\lambda} \, dB/cm \tag{4}$$

Where λ (μm) is the source wavelength and $Im(n_{eff})$ indicates the effective coupling mode RI imaginary part.

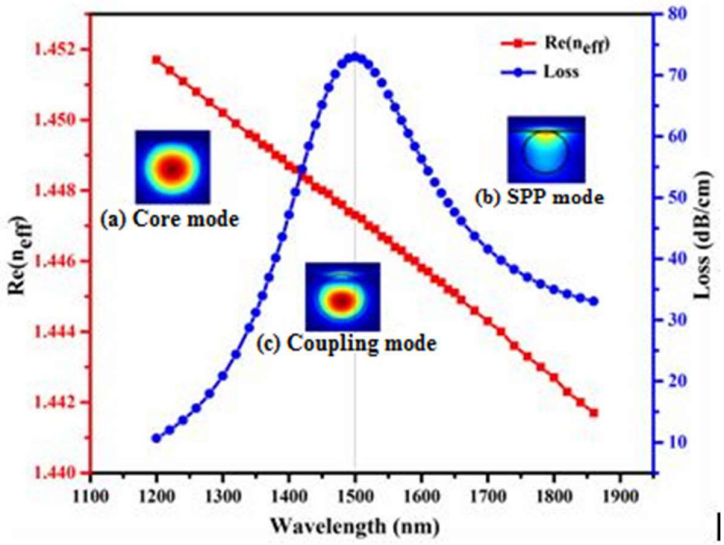

Fig. 4.3 Variation of real part RI and confinement loss spectra of coupling mode with wavelengths at analyte ($\boldsymbol{n_{am}}$) = 1.23, thickness of AZO layer (t) = 90 nm and width (w) = 124.57 μm.

The coupling mode RI imaginary part $Im(n_{eff})$ is related to the loss whereas the real part $Re(n_{eff})$ shows the RI in the usual sense. In Fig. (4.3), red curve shows the RI real part of the effective coupling mode that continuously decreasing with the wavelengths and the blue curve represents the confinement loss spectra variation with

wavelengths. This loss is determined by the imaginary part of the coupling mode effective RI using the Eq. (4.4). The loss spectrum is appeared an upward with higher value initially and decreasing with lower value after achieved the maximum loss peak at a resonant wavelength (1500 nm) at phase-matching coupling condition.

The characteristics of the sensor are determined by the different many performance parameter i.e. confinement loss, resonant wavelength, sensitivity and resolution. The surface plasmon wave is generated by the AZO plasmonic material and the thickness of the AZO layers affected the SPR phenomenon. Fig. 4.4 (a) exhibits confinement loss spectra curves for 30 nm to 90 nm thick AZO layers within the wavelength range from 1060 nm to 2660 nm for analyte RI 1.36. As shown in the figure, resonance loss peak increases with the thickness of the AZO layer in red-shift wavelength region.

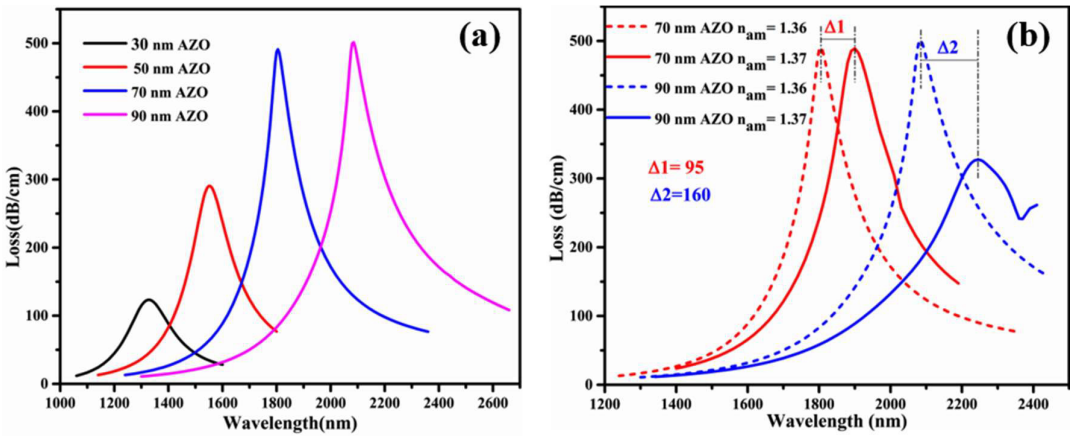

Fig. 4.4 (a) Change in loss spectra with wavelength for different thickness of AZO layers at analyte RI 1.36. **(b)** Loss spectra variation of sensor for 70 nm and 90 nm thick AZO layers at analyte RI 1.36 and 1.37.

Fig. 4.4 (b) shows that if analyte RI varies from 1.36 to 1.37, I are obtained resonant wavelengths shift values 95 nm and 160 nm for 70 nm and 90 nm thickness of AZO layer, respectively. Fig. 4.5 illustrates the confinement loss value spectra of sensor for various widths (40 µm, 60 µm, 80 µm, 100 µm, and 124.70 µm) of AZO layer for analyte RI 1.35

and 1.36. For analyte RI 1.35, we have obtained peak loss values 337.8482 nm/RIU, 337.7934 nm/RIU, 337.7386 nm/RIU, 337.7934 nm/RIU, and 337.7600 nm/RIU for 40 µm, 60 µm, 80 µm, 100 µm, and 124.70 µm width AZO layers at constant 1990 nm resonant wavelength, respectively. Also I have calculated peak loss values 501.4944 nm/RIU, 501.2850 nm/RIU, 501.0494 nm/RIU, 501.2588 nm/RIU, and 501.2588 nm/RIU for different width AZO layers 40 µm, 60 µm, 80 µm, 100 µm and 124.70 µm, respectively for another RI 1.36 at 2085 nm resonant wavelength. According to these data, resonant wavelength value is fixed and peak loss value only minor changes with the width of AZO layers.

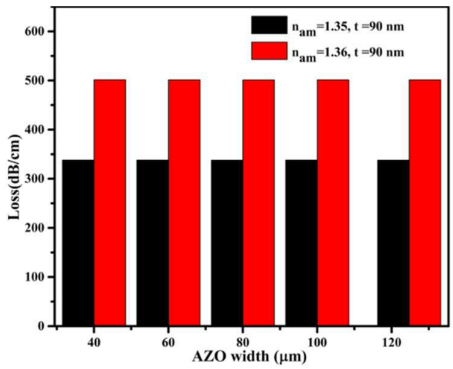

Fig. 4.5 Variation in losses with widths of AZO layers at fixed thickness (t) = 90 nm and analyte RIs n_{am}=1.35 and n_{am} =1.36.

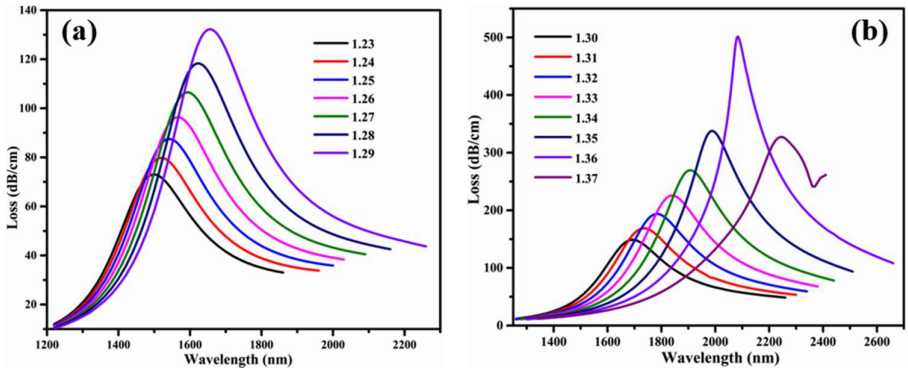

Fig. 4.6 Variation in loss spectra with wavelengths for different analyte RI **(a)** 1.23-1.29 **(b)** 1.30-1.37 at fixed thickness (t) = 90 nm and width (w) = 124.70 µm.

This D-shape SPR infrared sensor is more sensitive to the external medium RI. Fig. (4.6) describes the loss spectra variation of the infrared sensor for analyte RIs from 1.23 to 1.37 in wavelength range 1200 nm-2600 nm. The loss peak value increase with the analyte RIs due to strong coupling. I have obtained loss peak at resonant wavelength for different analyte RIs.

Fig. 4.7(a) shows the variation in resonance wavelength with the analyte RI for different thick AZO layers. I can see in figure, resonance wavelengths of sensor move to larger wavelength side with increases the refractive index of analyte for all thickness of the AZO layers. I have found higher value resonance wavelength for higher value analyte RI and lower value resonance wavelength for small value RI. It can be clarified by Eq. (4.3), the real value of propagation constant (K_{spw}) of SPW will be higher for a higher value of analyte RI. Hence its SPR condition is obtained at a larger wavelength. Similarly, for lower value of the analyte RI, the SPR condition is obtained at the lower wavelength due to the smaller real value of K_{spw} [105].

The sensitivity is significant parameter to examine the performance of the SPR based fibre sensor. The wavelength interrogation method is mostly used for long wavelength range and larger sensitivity SPR sensor. The wavelength sensitivity can be defined as follows Eq. (4.5) [170]

$$S_\lambda = \frac{\Delta\lambda_{peak}}{\Delta n_{am}} \ (nm/RIU) \tag{4.5}$$

Where $\Delta\lambda_{peak}$ represents the resonant wavelengths shift of two-loss peak and Δn_{am} indicates the change in two analyte RI medium.

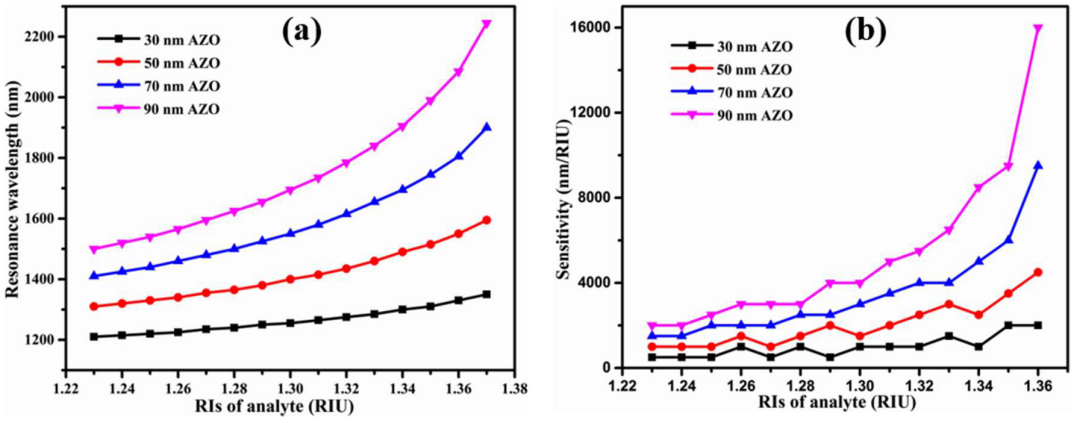

Fig. 4.7 Variations of the resonance wavelength and sensitivity with analyte RIs for different thickness of AZO layers.

Fig. 4.7(b) illustrates the sensitivity variations with the analyte RIs for 30 nm, 50 nm, 70 nm and 90 nm thick AZO layers. It explicates from this figure that the sensitivity of the proposed sensor enhances with a thickness of the AZO layers. For better performance, I have optimized a 90 nm thick AZO layer for my sensor. I have achieved maximum resolution 6.25×10^{-6} RIU of SPR sensor for analyte RIs 1.36-1.37 that is obtained by the following equation[171]

$$R = \frac{\Delta\lambda_{min}}{S_\lambda} \ (RIU) \tag{4.6}$$

Where $\Delta\lambda_{min}$ (= 0.1 nm) is the minimum wavelength instrumental resolution.

Table 4.2 Performance properties of SPR based D-shaped fiber sensor.

Analyte RI	Loss peak (dB/cm)	Resonance Wavelength (nm)	Peak shifting (nm)	Sensitivity (nm/RIU)	Resolution (RIU)
1.23	73.01	1500	20	2000	5.00×10^{-5}
1.24	79.81	1520	20	2000	5.00×10^{-5}
1.25	87.51	1540	25	2500	4.00×10^{-5}
1.26	96.34	1565	30	3000	3.33×10^{-5}
1.27	106.51	1595	30	3000	3.33×10^{-5}
1.28	118.32	1625	30	3000	3.33×10^{-5}
1.29	132.22	1655	40	4000	2.50×10^{-5}
1.30	148.74	1695	40	4000	2.50×10^{-5}
1.31	168.80	1735	50	5000	2.00×10^{-5}
1.32	193.65	1785	55	5500	1.81×10^{-5}
1.33	225.68	1840	65	6500	1.54×10^{-5}
1.34	269.46	1905	85	8500	1.18×10^{-5}
1.35	337.77	1990	95	9500	1.05×10^{-5}
1.36	501.26	2085	160	16000	6.25×10^{-6}
1.37	327.31	2245	NA	NA	NA

I have optimized 90 nm thick and 124.72 μm width AZO layer for my sensor. Table 4.2 shows the all performance properties of proposed sensor i.e. loss peak, resonance wavelength, peak shifting, sensitivity, and resolution. The loss peak values and resonance wavelengths of sensor are varies from 73.01 dB/cm to 327.31 dB/cm and 1500 nm to 2245 nm, respectively. Besides, the wavelength sensitivity of sensor varies from 2000 nm/RIU to 16000 nm/RIU for analyte RIs range 1.23-1.37. This RI range covers the many organic chemical, bio-chemical, different chemical mixtures and liquid food such as fluorine containing organics with various concentration, i.e. 1,1,1-trifluoroacetone (n_{am} < 1.30), 1,1,1,3,3,3-hexafluoro-2-propanol (n_{am} = 1.275), 2,2,2-trifluoroethyl trifluoroacetate (n_{am} = 1.2812), trifluoroacetic acid (n_{am} = 1.2850), 2,2,2-trifluoroethanol (n_{am} = 1.2907), heptafluorobutyric acid (n_{am} < 1.30), trifluoroacetic anhydride (n_{am} < 1.30) (Dean et al. 1998), savoflurane (n_{am} = 1.27) used in medical field for anesthetic[160], pure

honey (n_{am} = 1.356)[172] and other low RIs analyte. Table 4.3 shows the comparison my work with other author previous reported work.

Table 4.3 Performance comparison of low RI detection SPR sensor.

Reference	Type of sensor	Max. Sensitivity (nm/RIU)	Resolution (RIU)	RI range
173	PCF sensor	6000	2.80×10^{-5}	1.27-1.36
76	PCF sensor	10700	9.93×10^{-6}	1.19-1.29
174	PCF sensor	15000	6.67×10^{-6}	1.22-1.33
150	PCF sensor	13500	7.41×10^{-6}	1.27-1.32
175	PCF sensor	11055	9.05×10^{-6}	1.20-1.29
176	PCF sensor	10000	2.00×10^{-5}	1.35-1.40
177	Optical fibre sensor	3725	2.68×10^{-5}	1.27-1.33
132	Optical fibre sensor	10280	9.72×10^{-6}	1.33-1.38
178	Optical fibre sensor	10766.28	$9.29 \times 10\text{-}^{6}$	1.33-1.37
179	Experimental optical fibre sensor	70	5.90×10^{-5}	1.333-1.345
Proposed work	Optical fibre sensor	16000	6.25×10^{-6}	1.23-1.37

4.4 Fabrication methods and tolerance

I have calculated my designed sensor's results performance by the theoretically simulation analysis so experimental fabrication feasibility is mandatory for this sensor structure. The simulated investigation better results performances are not importance if the designed structure is no experimental fabrication. Hence, for my sensor device, I am suggesting the fabrication techniques. Initially, my requirement to construct the D-shaped optical fibre and then coat it with the Al-doped ZnO plasmonic material.

My sensor structure design is very simple so that it can be easily fabricated using the laser micro-machine and side-polishing techniques. These techniques are very simple and most convenient for controlling the depth of the fibre and fabrication of D-shaped fibre[180]. After constructing the D-shaped optical fibre structure, it needs to be coated with the Al-

doped ZnO plasmonic material for SPR condition. The optical fibre can be deposited using the many authentic techniques like as high-pressure micro-fluidic chemical deposition, chemical vapour deposition (CVD), electron beam evaporation, atomic layer deposition (ALD), wheel polishing, and liquid phase deposition (LPD)[181 182]. The thin Al-doped ZnO layers of my sensor are experimentally achievable by the different deposition techniques since Harith et al. proposed a relative humidity sensor with Al-doped ZnO layer which was coated by the sol-gel method[166]. So, I have discussed the about all fabrication methods that can construct my design sensor.

Although the current methods can be construct my structure device but a question is remaining that whether optical fibre sensor structure parameters dimensions can be exactly maintained in the experimental study. In the real scenario, when I am fabricating the device, then we generally face ±1-2 % changes in the optimized parameters (Al Mahfuz et al. 2020). I can be seen from Fig. 4.5 that the loss values almost constant and the resonant wavelength remain same with AZO layer width (w) variation therefore the sensor performance is unaffected by deviation of the AZO layer width. For ± 5% deviation of the thickness (t) from their optimized value, Ihave calculated the alteration of the sensor performance. Fig. 4.8 demonstrates the effect of AZO layer thickness (t) variation on the loss. I find the 8 nm shift in resonant wavelength for - 5% deviation in (t) and 7 nm shift in resonant wavelength for + 5% deviation. These small variations in resonant wavelength will have negligible effected on the sensor results. My structure can tolerate the ± 5% range fabrication error without any change in sensor results.

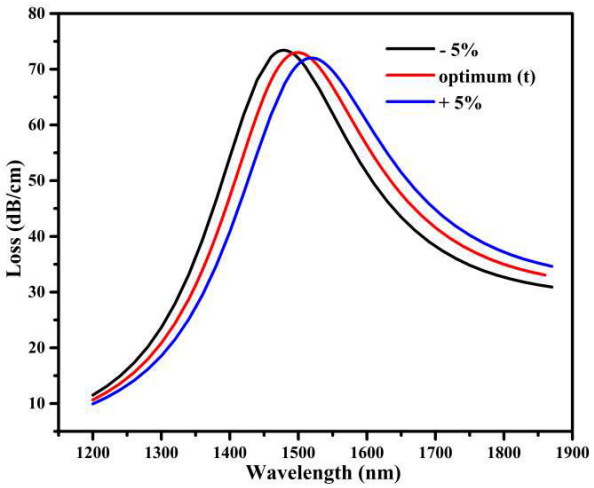

Fig. 4.8 Loss curve at RI 1.23 with ± 5% variation in AZO layer thickness (t).

4.5 Conclusion

The SPR principle based novel D-shape sensor is designed and it's numerically analysis by the finite element method (FEM) for low RI analyte detection has been made. For SPR condition, Al-doped ZnO (AZO) has been used as plasmonic material. My structure is easy to design as there is only single layer AZO coated on polished D-shape fiber. The proposed SPR sensor has achieved the wavelength sensitivity 2000-16000 nm/RIU for analyte RIs range 1.23 - 1.37 by adjusting the thickness of AZO layer. The maximum resolution is obtained 6.25×10^{-6} for analyte RIs range 1.36-1.37. The SPR sensor has high potential to detect low RI analyte i.e. drugs inspection and monitoring, biological and organic species and other analytes.